Solution Structure of Calmodulin bound to the target peptide of Endothelial Nitric Oxide Synthase phosphorylated at Thr495

Michael Piazza, Valentina Taiakina, Simon R. Guillemette, J. Guy Guillemette and Thorsten Dieckmann**

Department of Chemistry, University of Waterloo, Waterloo, Ontario N2L 3G1, Canada

[1] Funding Source Statement: This work was supported by the National Science and Engineering Research Council (NSERC) under grant no. 326911-2009 and 183521

[*] To whom correspondence should be addressed: University of Waterloo, Dept. of Chemistry, 200 University Ave West, Waterloo, ON, N2L3G1, Canada. E-mail: tdieckma@uwaterloo.ca; Fax: +1-519-7460435; Tel: +1-519-8884567

Abbreviations: NOS, Nitric oxide synthase; iNOS, inducible NOS; eNOS,endothelial NOS; nNOS, neuronal NOS; cNOS,constitutive NOS; CaM, Calmodulin; NMR, Nuclear magnetic resonance; CaM-eNOS, CaM-eNOS binding domain peptide; CaM-eNOSpThr495, CaM-eNOS binding domain peptide with phosphorylated Thr495; PDB, Protein data bank; RMSD, root mean square deviation; NOE, Nuclear Overhauser Enhancement; NOESY, nuclear Overhauser effect spectroscopy; TOCSY, total correlation spectroscopy; HSQC, heteronuclear single-quantum coherence; ITC, Isothermal Titration Calorimetry; CD, Circular Dichroism; TFE, Trifluoro ethanol.

ABSTRACT: Nitric oxide synthase (NOS) plays a major role in a number of key physiological and pathological processes and it is important to understand how this enzyme is regulated. The small acidic calcium binding protein, calmodulin (CaM), is required to fully activate the enzyme. The exact mechanism of how CaM activates NOS is not fully understood at this time. Studies have shown CaM to act like a switch that causes a conformational change in NOS to allow for the electron transfer between the reductase and oxygenase domains through a process that is thought to be highly dynamic and at least in part controlled by several possible phosphorylation sites. We have determined the solution structure of CaM bound to a peptide that contains a phosphorylated threonine corresponding to Thr495 in full size eNOS in order to investigate the structural and functional effects that the phosphorylation of this residue may have on nitric oxide production. Our biophysical studies show that phosphorylation of Thr495 introduces electrostatic repulsions between the target sequence and CaM as well as a diminished propensity for the peptide to form an α-helix. The calcium affinity of the CaM-target peptide complex is reduced due to phosphorylation and this leads to weaker binding under low physiological calcium concentrations. This study provides an explanation for the reduced NO production by eNOS carrying a phosphorylated Thr495 residue.

Nitric oxide synthase (NOS) enzymes (E.C. 1.14.13.39) catalyze the production of nitric oxide (•NO) that acts as a secondary inter- and intracellular messenger involved in many physiological processes.[1] Three NOS isozymes are found in mammals: neuronal NOS (nNOS, NOS I), endothelial NOS (eNOS, NOS III), and inducible (iNOS, NOS II). The NOS enzymes are homodimeric with each monomer containing an *N*-terminal oxygenase domain, which contains binding sites for the catalytic heme, tetrahydrobiopterin (H_4B), and the substrates L-arginine and molecular oxygen, and a *C*-terminal reductase domain, which contains binding sites for the cofactors FMN, FAD, and NADPH. A Calmodulin (CaM) binding domain connects the oxygenase and reductase domains and is required for efficient electron transfer from the reductase to the oxygenase domain for •NO production.[1,2] CaM binds and activates the Ca^{2+}-dependent constitutive NOS (cNOS) enzymes, eNOS and nNOS, at elevated cellular Ca^{2+} concentrations, whereas, iNOS is transcriptionally controlled *in vivo* by cytokines and binds to CaM in a Ca^{2+}-independent manner. A large conformational change that CaM induces in the reductase domain of the NOS enzymes allows for the FMN domain to interact with the FAD to accept electrons and pass the electrons on to the heme during catalysis.[3] Clearly, these conformational changes caused by CaM are important in stimulating efficient electron transfer within the NOS enzymes.

CaM is a ubiquitous cytosolic Ca^{2+}-binding protein that is able to bind and regulate hundreds of different intracellular proteins.[4] CaM consists of two globular domains joined by a flexible central linker region. Each domain contains two EF hand pairs that are each capable of binding one Ca^{2+} ion. The binding of Ca^{2+} to CaM causes a conformational change which exposes hydrophobic patches that allow it to associate with its intracellular target proteins. The flexibility of CaM's central linker separating the *N*- and C-domains allows it to adapt its conformation to

optimally associate with its intracellular targets.[5,6] Both the N- and C-lobes must be calcium replete to fully activate eNOS and nNOS enzymes.[7,8]

eNOS activity is regulated by multiple mechanisms, including posttranslational modifications such as protein phosphorylation.[9,10] The binding of CaM and the transfer of electrons from the reductase to the oxygenase domain of eNOS is dependent on protein phosphorylation and dephosphorylation.[9] eNOS can be phosphorylated on serine, tyrosine and threonine residues and contains many potential phosphorylation sites that can play a role in regulating its activity.[11–14] Phosphorylation of Ser1177 in the reductase domain has been found to result in the activation of eNOS, whereas the phosphorylation of Thr495 within the CaM-binding domain has been found to reduce eNOS activity.[15–17] Perturbations of eNOS phosphorylation have been reported in a number of diseases.[18] Phosphorylation of Thr495 acts as a negative regulatory site and has been reported to interfere with the binding of CaM to the CaM-binding domain affecting activation of the enzyme.[9,15]

There is considerable interest in understanding the structural and functional effects that the phosphorylation of Thr495 in eNOS has on the calcium dependent CaM binding and activation of the enzyme. In the present study the structural and functional effects that the phosphorylation of eNOS has on binding to CaM were investigated. Steady-state fluorescence and isothermal titration calorimetry (ITC) were used to monitor the binding of CaM to the wild type eNOS CaM-binding region peptide and the eNOS CaM-binding region peptide phosphorylated at Thr495 at various free Ca^{2+} concentrations. The structural effects of Thr495 phosphorylation on CaM binding to eNOS were investigated by the determination of the solution structure of CaM bound to the eNOS CaM-binding region peptide phosphorylated at Thr495. This investigation

provides a better understanding of the interaction of CaM with the phosphorylated or nonphosphorylated CaM-binding region of eNOS at Thr495.

EXPERIMENTAL PROCEDURES

CaM Protein Expression and Purification. Wild-type CaM protein was expressed and purified using phenyl sepharose chromatography, as previously described.[7] Isolation of the CaM proteins (148 residues) was confirmed by ESI-MS and purity was judged to be > 95% by SDS-PAGE. The human eNOS (TRKKTFKEVANAVKISASLMGT, 22 residues corresponding to residues 491-512 from the full length eNOS protein) peptide was synthesized and purchased from Sigma. The Thr495 phosphorylated human eNOS (TRKKpTFKEVANAVKISASLM, 20 residues corresponding to residues 491-510 from the full length eNOS protein) peptide was synthesized and purchased from GenScript. The phosphorylation was confirmed by ESI-MS.

Sample Preparation for NMR Investigation. CaM for NMR experiments were expressed in M9 media (11.03 g/L $Na_2HPO_4 \cdot 7H_2O$, 3.0 g/L KH_2PO_4, 0.5 g/L NaCl, 2 mM $MgSO_4$, 0.1 mM $CaCl_2$, 5 mg/mL Thiamine, 100 μg/mL kanamycin) containing 2 g/L ^{13}C-glucose and 1 g/L $^{15}NH_4Cl$. ^{13}C-^{15}N CaM was purified as described above. The samples were prepared for NMR experiments via a buffer exchange into NMR solution (100 mM KCl, 10 mM $CaCl_2$, 0.2 mM NaN_3, 90% H_2O/10% ^2H_2O) at pH 6.0 using a YM10 centrifugal filter device (Millipore Corp., Billerica, USA). All NMR samples contained at least 1 mM CaM in a total volume of 500 μL. The samples were transferred into 5 mm NMR sample tubes and stored at 4°C until required for NMR experiments. NMR experiments on the complexes were conducted on CaM samples titrated with eNOSpT495 peptide to saturation in a 1:1 CaM:peptide ratio. Complex formation was monitored after each addition by acquisition of a ^1H-^{15}N heteronuclear single-quantum coherence (HSQC) spectrum.

NMR Spectroscopy and Data Analysis. NMR spectra were recorded at 25ºC on Bruker 600 and 700 MHz DRX spectrometers equipped with XYZ-gradients triple-resonance probes (Bruker, Billerica, MA, USA). Spectra were analyzed using the program CARA (Computer Aided Resonance Assignment).[19]

Specific assignments of the CaM backbone resonances were achieved using a combination of 3D triple resonance experiments including HNCA, HN(CO)CA, CBCA(CO)NH, and HNCO.[20,21] Side-chain resonances were assigned using the TOCSY type experiments HC(C)H-TOCSY, (H)CCH-TOCSY and H(CCO)NH.[22] Specific assignments of the eNOSpThr495 peptide were obtained from ^{15}N-double-filtered NOESY experiments (Figure S.1).[23]

Structure Calculation. The ^{1}H, ^{13}C and ^{15}N resonance assignments were utilized to identify constraints for the structure calculations. Distance constraints for the solution structure of CaM-eNOSpThr495 were obtained from ^{15}N-NOESY-HSQC, ^{13}C- NOESY-HSQC and ^{15}N-double-filtered NOESY spectra acquired on samples containing labeled CaM and unlabeled peptide.[23–25] In addition, dihedral angle restraints were derived from chemical shift analysis with TALOS+.[26] CNSsolve version 1.2[27] was used to perform the structure calculations using standard simulated annealing protocols.

Delphi Calculation of the CaM Structures. Delphi electrostatic potentials of the structure was calculated using the DelPhiController interface of UCSF Chimera 1.5.3 (build 33475).[28] The parseRes atomic radii file and atomic charge file were used as the input files in the calculation. The electrostatic potential surface was visualized in Chimera.

Dansylation of CaM. Dansyl-CaM was prepared as previously described.[29] CaM (1 mg/ml) was buffer exchanged into 10 mM $NaHCO_3$, 1 mM EDTA, pH 10.0, at 4°C. 30 µl of 6 mM dansyl-chloride (1.5 mol/mol of CaM) in DMSO was added to 2 ml of CaM, with stirring. After

incubation for 12 hr at 4°C, the mixture was first exhaustively dialyzed against 500 volumes of 150 mM NaCl, 1 mM EDTA, 20 mM Tris-HCl, pH 7.5, at 4°C, then exhaustively dialyzed against 500 volumes of water. Labeling yields were determined from absorbance spectra using the ε_{320} of 3,400 $M^{-1}cm^{-1}$ and were compared to actual protein concentrations determined using the Bradford method with wild-type CaM used as the protein standard.[30] ESI-MS was used to confirm successful dansyl-labeling of each CaM protein. The concentration of dansyl-CaM in all experiments was 2 μM.

Steady State Fluorescence. Fluorescence emission spectra were obtained using a PTI QuantaMaster spectrofluorimeter (London,ON). Fluorescence measurements were made on 50 μL samples consisting of dansyl-CaM (2 μM) alone or with eNOS or eNOSpThr495 peptide in 30 mM MOPS, 100 mM KCl, 10 mM EGTA, pH 7.2 with an increasing concentration of free Ca^{2+}. Free Ca^{2+} concentration was controlled using the suggested protocol from the calcium calibration buffer kit from Invitrogen. The excitation wavelength for all of the dansyl-CaMs was set at 340 nm and emission was monitored between 400 and 600nm. Slit widths were set at 2 nm for excitation and 1 nm for emission. Relative fluorescence was calculated by the following equation: relative fluorescence = $(F - F_0)/(F_{max} - F_0)$, where F is the measured intensity, F_{max} is the maximum intensity, and F_0 is the intensity without added Ca^{2+}.

Isothermal Titration Calorimetry. All ITC recordings were performed on a Microcal ITC200 from Microcal (Northampton, MA) at 25°C, 1000 rpm stir speed, and reference power set to 5 μcal/s. In the experiments at saturating Ca^{2+} concentrations the buffer used was 30 mM MOPS, 100 mM KCl, pH 7.2 and 1 mM $CaCl_2$ and was identical between cell and syringe. In the experiments at 225 nM free Ca^{2+} the calcium calibration buffer kit from Invitrogen was used and the buffer consisted of 15 mM MOPS, 50 mM KCl, pH 7.2 10 mM EGTA and 6.0 mM

CaEGTA and was identical between cell and syringe. Buffer into buffer, peptide into buffer and buffer into CaM controls showed no significant baseline decay or drift and relatively low, consistent heats of injection, indicating sufficiently matched cell and syringe buffer conditions.. 39 μL of each peptide was titrated into 200 μL of CaM at varying concentrations (optimal starting conditions were determined empirically), typically from 100 μM peptide into 10 μM CaM to 500 μM peptide into 50 μM CaM, over the course of 20–30 injections at 2–3 min intervals. Data analysis was performed using Origin ITC200 Origin70 module with pre-loaded fitting equations for one- and two-sites models. The one-set-of-sites model was found to be applicable to all experiments.

Circular Dichroism (Spectropolarimetry). CD was performed using a Jasco J-715 CD spectropolarimeter and analyzed using J-715 software(Jasco Inc., Easton, MD, USA) as previously described (Fernando et al., 2002) with some modifications. Samples were measured in a 1 mm quartz cuvette (Hellma, Concord, ON) and kept at 25°C using a Peltier type constant-temperature cell holder (model PFD 3505, Jasco, Easton, MD). Samples consisted of 10 μM of synthetic eNOS or phosphorylated eNOS (peNOS) CaM-binding domain peptides. Samples were in 10 mM Tris-HCl buffer (pH 7.5), 150 mM NaCl, containing 200 μM $CaCl_2$ followed. Spectra were recorded over a 190-250 nm range with a 1.0 nm band width, 0.2 nm resolution, 100 mdeg sensitivity at a 0.125 s response and a rate of 100 nm/min with a total of 25 accumulations. Data is expressed as the mean residue ellipticity (**θ**) in degree cm^2dmol^{-1}.

Accession Numbers. The coordinates and NMR parameters for the 'Solution Structure of Calmodulin bound to the target peptide of Endothelial Nitrogen Oxide Synthase phosphorylated at Thr495' have been deposited in the PDB and BMRB and have been assigned RCSB ID code rcsb103588, Protein Data Bank (PDB) ID code 2mg5 and BMRB accession number 19586.

RESULTS AND DISCUSSION

CD and NMR Spectroscopy. NMR spectroscopy was used to assess changes to the CaM-eNOS complex due to the phosphorylation of Thr495. Figure 1a shows the overlay of the ^{15}N-HSQC spectra of CaM-eNOS with that of CaM-eNOSpThr495. Cross peaks for the majority of amides in the CaM-eNOSpThr495 complex overlap with those of CaM-eNOS complex. However, amides in the *C*-domain, specifically the amides of residues in EF hand IV, do not overlap with those of CaM-eNOS due to differences in chemical shifts. Also not seen in Figure 1a is the chemical shift difference of E7, which is located in the heavily overlapped central portion of the spectra. This data suggests that the structures of the CaM-eNOS complex and the CaM-eNOSpThr495 complex are quite similar. This provides further evidence that this phosphorylation affects residues E7 and E127, which are in close proximity to the phosphorylated Thr495 in the structure. This has been previously postulated by Aoyagi et al. when they suggested that the addition of a negatively charged phosphate group would cause electrostatic repulsion between E7 and E127.[31]

The effect of phosphorylation on the secondary structure of the peptide was investigated using trifluoroethanol (TFE) monitored by circular dichroism spectroscopy. The TFE is used to mimic hydrophobic environments and is known to induce α-helical conformation in peptides that have a propensity to form this secondary structure. Both eNOS peptides showed no apparent structure in the buffer solution with 0% TFE. A comparison of the tendency of each peptide to form an α-helix was then performed by recording spectra after the addition of increasing concentrations of TFE. The formation of an α-helix is generally accompanied by the appearance of negative ellipticity at 208 and 222 nm. Both peptides showed increased amounts of secondary structure as

more TFE was added. In both cases, there was an increase in apparent α-helical structure with increasing TFE concentration. With increasing concentrations of TFE, the negative ellipticity at 222 nm of both peptides plateau at TFE concentrations above 30% (see Figure 1b). While this result indicates that the increase in helical structure does not appreciably change above 30% TFE, the phosphorylated peptide did not show as large an α-helical content as the nonphosphorylated peptide (Figure 1b). The structural effects of the phosphorylation leading to the diminished helical structure of the peptide can be due to the charged and bulky nature of the phosphate, destabilization of electrostatics that can result in nonproductive interaction with neighboring residues or the high desolvation penalty of the side chain.[32] Specifically, it has been previously proposed that phosphorylation at Thr495 OG1 would disrupt its hydrogen bond with the Glu498 backbone amide, possibly affecting the α-helical secondary structure of the peptide.[31] In addition, the Thr495 is next to one of the anchoring residues in the classical '1-5-8-14' CaM binding sequence motif. A negatively charged phosphorylated Thr495 next to the first residue of the motif will likely disrupt the helical structure of the region.

While the propensity of the phosphorylated eNOS CaM binding domain to form an α-helix appears to be diminished, the final structure of the peptide bound to CaM is very similar to that of the nonphosphorylated form of the peptide. The diminished α-helical propensity could account for the reduced activity of the enzymes associated with the phosphorylated form.

Structure of CaM-eNOSpThr495 CaM Binding Peptide Complex. The three dimensional solution structure of CaM bound to the human eNOS CaM binding domain peptide phosphorylated at Thr495 (CaM-eNOSpThr495) was determined using multi-dimensional heteronuclear NMR spectroscopy. The structure of the complex is based on a large number of experimental constraints and is well defined. Structure and input data statistics are summarized

in Table 1. The family of 20 final structures is shown in Figure 2a. The average structure showing the location of the phosphorylation of Thr495 of the eNOS peptide, which is found near the N-terminal end of the peptide is shown in Figure 2b. Residues 1-4 (corresponding to 491-494 of eNOS) at the *N*-terminus of the eNOSpThr495 CaM binding region peptide were not included in the structure calculation because they could not be unambiguously assigned. This could be due to the addition of the phosphate group which has been theorized to destabilize the helical propensity of the peptide.[31] Based on the comparison of the ^{15}N-double filtered NOESY experiments for CaM with eNOS peptide and CaM with eNOSpThr495 peptide there was little change in the chemical shifts observed for pThr495 and Thr495.

Comparison of the CaM-eNOS vs CaM-eNOSpThr495 Complexes. When the solution structure of CaM-eNOS is superimposed onto that of the CaM-eNOSpThr495 structure, the two structures are shown to be quite similar, however, a few local differences are seen (Figure 3). When aligned with respect to the backbone atoms of the peptide, a difference is shown in the orientation of helix A of CaM between the two structures, with helix A of CaM-eNOSpThr495 pushed away from the N-terminus of the peptide (where the phosphorylated Thr495 is located). EF hand IV (colored blue) is also shifted farther away from the peptide in the CaM-eNOSpThr495 structure. The rest of the CaM-eNOSpThr495 structure superimposes quite well on the CaM-eNOS structure. This, along with the ^{15}N-HSQC spectra overlay, confirms that the phosphorylation of Thr495 doesn't have an effect on the structure of CaM away from the site of the phosphorylation.

Electrostatic Effects of the Phosphorylation of Thr495. The addition of the phosphate group to Thr495 of the eNOS peptide shows structural effects on EF hands I and IV. This is first illustrated by the ^{15}N-HSQC spectra overlay of the CaM-eNOS and CaM-eNOSpThr495

complexes (Figure 1a) and is clearly shown by the structure overlay of the two structures (Figure 3). The analysis of the CaM-eNOSpThr495 structure with DelPhi illustrates that this modification to the peptide creates a more negative potential on the N-terminal region of the peptide, which is located in a negatively charged region of CaM (Figure 4b, d). This negative charge is not present in the CaM-eNOS complex (figure 4c) and thus would not cause any electrostatic repulsion. This phosphate group is in close proximity to E7, which is found in helix A of EF hand I, and E127, found in helix G of EF hand IV. The electrostatic repulsion between the phosphate group and helix A of EF hand I gives an explanation as to why helix A is pushed further from the peptide in the CaM-eNOSpThr495 complex, as shown in Figure 3. This also explains why helix G and EF hand IV are shifted further away from the eNOSpThr495 peptide. This electrostatic repulsion could be affecting CaM's ability to coordinate Ca^{2+} by interfering with the EF hands I and IV, which would help explain why CaM has diminished ability to bind eNOS phosphorylated at Thr495 at physiological Ca^{2+} levels.

Fluorescence Spectroscopy Suggests Increased Ca^{2+} Sensitivity of CaM with the eNOS Peptide. Binding of the eNOS and eNOSpThr495 peptides with CaM was further studied using dansylated CaM (dansyl-CaM). Dansyl-CaM is a useful tool to detect conformational changes in CaM as a result of interactions with Ca^{2+}, peptides or other proteins because the intensity of the fluorescence spectrum is enhanced and shifted when the dansyl moiety becomes embedded in a hydrophobic environment.[29,33] Without Ca^{2+} present there was no blue shift or enhancement of dansyl fluorescence spectrum observed when eNOS peptide or eNOSpThr495 peptide were added. In the presence of Ca^{2+}, this shift and enhancement of the fluorescence spectrum was observed. To analyze the Ca^{2+} dependency of the two complexes we performed Ca^{2+} titration fluorescence experiments in triplicate (Figure 5). Without peptides, dansyl-CaM exhibited

fluorescence changes in a Ca^{2+} concentration range of 0.35-2.8 μM. The fluorescence changes of the dansyl-CaM-eNOS complex occurred in a much lower Ca^{2+} concentration range, which may correspond to a physiological Ca^{2+} concentration. The dansyl-CaM-eNOSpThr495 complex showed no difference in Ca^{2+} dependency when compared to CaM alone. These Ca^{2+} titration experiments provide information about the conformational transitions of CaM with the peptides and Ca^{2+}. The result of the CaM-eNOS complex binding with Ca^{2+} at lower Ca^{2+} concentrations than CaM alone indicate that the Ca^{2+} affinity of CaM is enhanced with peptide binding to CaM. This is not seen in interaction of CaM with eNOSpThr495 peptide. This increased Ca^{2+} sensitivity of CaM have also been seen with other peptides interacting with CaM.[34] This suggests that binding of eNOS peptide to CaM increases the Ca^{2+} sensitivity of CaM in the physiological Ca^{2+} range, whereas eNOSpThr495 does not.

Isothermal titration calorimetry. Isothermal titration calorimetry (ITC) was used to examine the thermodynamic profiles associated with the binding CaM to the two target peptides. Since the values obtained for binding constants show slight variations when performed using different methods and conditions,[35,36] all of our experiments were performed by ITC using exactly the same conditions. Representative titrations for each are shown in figure 6. In the presence of excess calcium (1mM) wild type eNOS peptide binds to CaM by an exothermic interaction. As previously reported for the binding of the nNOS peptide,[37] eNOS binding proceeds with a negative enthalpy (ΔH) and a positive entropy (ΔS) and modest affinity (K_d = 0.7μM). This indicates that the interaction is driven by favorable enthalpy and entropy. In contrast, the binding of the eNOSpThr495 peptide under the same conditions is weakly endothermic, with a comparable affinity to that of wild type (K_d = 0.3μM). A similar endothermic interaction has been reported for apoCaM titrated with mutant peptides corresponding to the CaM binding

domain of iNOS, an isoform that is known to bind to CaM in the absence of calcium.[38] The eNOSpThr495 binding interaction proceeds with positive ΔH and ΔS. The interaction is therefore driven by the increase in entropy. Both peptides showed a 1:1 stoichiometry with CaM as expected.

Since our fluorescence studies showed an apparent difference in binding at low calcium concentrations, we attempted to thermodynamically characterize the interactions under these conditions. Intriguingly, at low $[Ca^{2+}]_{free}$, the binding of wild type eNOS peptide to CaM becomes highly endothermic, the entropy gain increases over fourfold, and its affinity for CaM increases slightly (K_d = 0.2μM). A similar result showing a switch from an exothermic to an endothermic interaction has been reported for the binding of the nNOS CaM target domain to CaM by simply changing the experimental conditions going from a higher to a lower temperature.[37] The ΔH under low 225nM calcium conditions is now positive and unfavorable for binding. The change in enthalpy is compensated by a much larger positive ΔS than that observed for the wild type peptide binding in excess calcium. In contrast, the binding of eNOSpThr495 to CaM in these low $[Ca^{2+}]_{free}$ conditions becomes negligible (Figure 6). This is consistent with our fluorescent experiments showing no apparent binding under these conditions. In essence, these results indicate that non-phosphorylated eNOS is more sensitive to ambient cellular Ca^{2+}, and phosphorylation serves as an attenuator of Ca^{2+}-CaM regulation of eNOS.

We set out to understand how phosphorylation of a single residue in the CaM target domain results in diminished NOS enzyme activity. Previous studies had shown that an eNOS enzyme carrying a phosphomimetic mutation T495D binds very weakly to CaM. In contrast, the control mutant T495A showed strong binding to CaM.[15] Enzyme studies also showed that only phosphorylation of T495 or the mutation T495D resulted in the loss of eNOS enzyme activity. It

had been postulated that phosphorylation of T495 reduces output by hindering the association of CaM with its binding site.[31] Until the present study, there had not been a structural study using a phosphorylated T495 residue. Our solution structure shows that in the presence of excess calcium, phosphorylation does not prevent the binding of CaM to the phosphorylated peptide. While the exact mechanism of how phosphorylation of Thr495 in eNOS adversely affects the activation of the enzyme is still unknown, a careful look at the complex does provide some idea of the reported cause for the reduced enzyme activity. A comparison of the two structures in figures 1 and 2 show that the most significant changes in the pThr495 solution structure involved two CaM amino acids E7 and E127. In addition both E11 and M124 are found to be in close proximity to the pThr495 phosphate group. The previously reported crystal structure of CaM bound to the human eNOS peptide shows that the side chains of these amino acids are in contact with a number of amino acids in the eNOS peptide.[31] Both E7 and E11 are part of helix A of the EF hand 1 in CaM. The E7 side chain is in contact with eNOS residues K497 and E498 and has ionic interactions with R492. The E11 side chain is in contact with eNOS residues E498, A502 and I505 and has a hydrogen bond with N501. Our results shown in Figure 3 indicate that helix A is pushed away from the peptide likely due to electrostatic repulsion.

The M124 and E127 residues are both in helix G of EF hand 4 in CaM. The side chain of M124 is in contact with eNOS residues T495, F496 and V499. Residue E127 of CaM has contact with T495 and K497. In addition E127 has ionic interactions with K493 and the backbone of T496. Electrostatic repulsion could again account for the displacement of helix G of EF hand 4 away from the peptide (Figure 3). Looking closely at the Delphi image with the phosphate present, the phosphorylation of Thr495 adds a negative charge that is close to helix G (Figure 4). The displacement of helix A and G may not be significant under conditions with 1 mM calcium,

but under physiological low calcium concentration conditions, a more significant displacement of these helices may have a detrimental effect on enzyme binding and activation. This comes from our dansyl-CaM experiments showing that the pThr495 peptide required significantly higher concentrations of calcium to bind to CaM. Our calorimetric study also showed a lack of binding of CaM to the phosphorylated peptide in the presence of 225nM free calcium. We used TFE to induce α-helical formation and used spectropolarimetry to monitor the changes in the secondary structure of the two eNOS peptides. The secondary structure of both peptides plateaus in 30% TFE but phosphorylation appears to result in a reduction in the degree of α-helical structure in the peptide. In the presence of high concentrations of calcium, the solution structure shows that both peptides form an α-helical structure when bound to CaM.

In summary, the interactions of CaM with the peptides based on the eNOS CaM binding domain or the eNOS CAM binding domain phosphorylated at Thr495 are very similar at saturating Ca^{2+} concentrations. This is confirmed by our NMR spectroscopy (see Figure S2,), fluorescence and ITC results. At the lower Ca^{2+} concentration of 225nM, near physiological Ca^{2+} levels, no significant binding of CaM to eNOSpThr495 is observed by either method, whereas CaM is binding to nonphosphoryated eNOS. When Thr495 is phosphorylated, our results indicate there is a diminished propensity for the formation of an α-helix by the peptide in combination with electrostatic repulsion that may account for the diminished CaM-dependent activation of the eNOS enzyme under low physiological calcium concentrations.

ACKNOWLEDGEMENTS. Molecular graphics images were produced using the UCSF Chimera package from the Resource for Biocomputing, Visualization, and Informatics at the University of California, San Francisco. DelPhi is supported by a funding from the National Science Foundation Grant # DBI-9904841.

SUPPORTING INFORMATION AVAILABLE. ^{15}N-double filtered NOESY spectrum of CaM with the eNOSpThr495 peptide bound, Overlay of ^{1}H-^{15}N HSQC spectra of CaM and CaM-eNOS peptide complex at 225nM free Ca^{2+}, Overlay of ^{1}H-^{15}N HSQC spectra of CaM and CaM-eNOSpThr495 peptide complex at 225nM free Ca^{2+}. This material is available free of charge via the Internet at http://pubs.acs.org

REFERENCES

(1) Alderton, W. K., Cooper, C. E., and Knowles, R. G. (2001) Nitric oxide synthases: structure, function and inhibition. *Biochem. J. 357*, 593–615.

(2) Daff, S. (2010) NO synthase: structures and mechanisms. *Nitric Oxide 23*, 1–11.

(3) Welland, A., and Daff, S. (2010) Conformation-dependent hydride transfer in neuronal nitric oxide synthase reductase domain. *FEBS J. 277*, 3833–3843.

(4) Ikura, M., and Ames, J. B. (2006) Genetic polymorphism and protein conformational plasticity in the calmodulin superfamily: two ways to promote multifunctionality. *Proc. Natl. Acad. Sci. U. S. A. 103*, 1159–1164.

(5) Persechini, a, and Kretsinger, R. H. (1988) The central helix of calmodulin functions as a flexible tether. *J. Biol. Chem. 263*, 12175–12178.

(6) Spratt, D. E., Israel, O. K., Taiakina, V., and Guillemette, J. G. (2008) Regulation of mammalian nitric oxide synthases by electrostatic interactions in the linker region of calmodulin. *Biochim. Biophys. Acta 1784*, 2065–2070.

(7) Spratt, D. E., Newman, E., Mosher, J., Ghosh, D. K., Salerno, J. C., and Guillemette, J. G. (2006) Binding and activation of nitric oxide synthase isozymes by calmodulin EF hand pairs. *FEBS J. 273*, 1759–1771.

(8) Spratt, D. E., Taiakina, V., Palmer, M., and Guillemette, J. G. (2007) Differential binding of calmodulin domains to constitutive and inducible nitric oxide synthase enzymes. *Biochemistry 46*, 8288–8300.

(9) Fleming, I., and Busse, R. (2003) Molecular mechanisms involved in the regulation of the endothelial nitric oxide synthase. *Am. J. Physiol. Regul. Integr. Comp. Physiol. 284*, R1–12.

(10) Piazza, M., Futrega, K., Spratt, D. E., Dieckmann, T., and Guillemette, J. G. (2012) Structure and Dynamics of Calmodulin (CaM) Bound to Nitric Oxide Synthase Peptides: Effects of a Phosphomimetic CaM Mutation. *Biochemistry 51*, 3651–3661.

(11) Fleming, I., Bauersachs, J., Fisslthaler, B., and Busse, R. (1998) Ca2+-Independent Activation of the Endothelial Nitric Oxide Synthase in Response to Tyrosine Phosphatase Inhibitors and Fluid Shear Stress. *Circ. Res. 82*, 686–695.

(12) Michell, B. J., Chen Zp, Tiganis, T., Stapleton, D., Katsis, F., Power, D. a, Sim, a T., and Kemp, B. E. (2001) Coordinated control of endothelial nitric-oxide synthase phosphorylation by protein kinase C and the cAMP-dependent protein kinase. *J. Biol. Chem. 276*, 17625–17628.

(13) Harris, M. B., Ju, H., Venema, V. J., Liang, H., Zou, R., Michell, B. J., Chen, Z. P., Kemp, B. E., and Venema, R. C. (2001) Reciprocal phosphorylation and regulation of endothelial nitric-oxide synthase in response to bradykinin stimulation. *J. Biol. Chem. 276*, 16587–16591.

(14) Kou, R., Greif, D., and Michel, T. (2002) Mechanisms of Signal Transduction : Dephosphorylation of Endothelial Nitric-oxide Synthase by Vascular Endothelial Growth

Factor : Implications for the Vascular Responses to Cyclosporin A. *J. Biol. Chem. 277*, 29669 – 29673.

(15) Fleming, I., Fisslthaler, B., Dimmeler, S., Kemp, B. E., and Busse, R. (2001) Phosphorylation of Thr495 Regulates Ca2+/Calmodulin-Dependent Endothelial Nitric Oxide Synthase Activity. *Circ. Res. 88*, e68–e75.

(16) Tran, Q.-K., Leonard, J., Black, D. J., and Persechini, A. (2008) Phosphorylation within an autoinhibitory domain in endothelial nitric oxide synthase reduces the Ca(2+) concentrations required for calmodulin to bind and activate the enzyme. *Biochemistry 47*, 7557–7566.

(17) Matsubara, M. (2003) Regulation of Endothelial Nitric Oxide Synthase by Protein Kinase C. *J. Biochem. 133*, 773–781.

(18) Kolluru, G. K., Siamwala, J. H., and Chatterjee, S. (2010) eNOS phosphorylation in health and disease. *Biochimie 92*, 1186–1198.

(19) Keller, R. (2005) Optimizing the Process of Nuclear Magnetic Resonance Spectrum Analysis and Computer Aided Resonance Assignment. Swiss Federal Institute of Technology.

(20) Grzesiekt, S., and Bax, A. (1992) Correlating Backbone Amide and Side Chain Resonances in Larger Proteins by Multiple Relayed Triple Resonance NMR. *J. Am. Chem. Soc. 114*, 6291–6293.

(21) Muhandiram, D. R., and Kay, L. E. (1994) Gradient-enhanced triple-resonance 3-dimensional NMR experiments with improved sensitivity. J. *J. Magn. Reson. 103*, 203–216.

(22) Bax, A., Clore, M., and Gronenborn, A. M. (1990) 1 H- 1 H Correlation via Isotropic Mixing of 13C a New Three-Dimensional Approach for Assigning lH and 13C Spectra of 13C-Enriched Proteins. *J. Magn. Reson. 88*, 425–431.

(23) Ikura, M., and Bax, A. (1992) Isotope-Filtered 2D NMR of a Protein-Peptide Complex Study of a Skeletal Muscle MLCK Fragment Bound to Calmodulin. *J. Am. Chem. Soc.* 2433–2440.

(24) Clore, G. M., and Gronenborn, A. M. (1991) Applications of three- and four-dimensional heteronuclear NMR spectroscopy to protein structure determination. *Prog. Nucl. Magn. Reson. Spectrosc. 23*, 43–92.

(25) Fesik, S. W., and Zuiderweg, E. R. P. (1990) Heteronuclear 3-Dimensional Nmr Spectroscopy Of Isotopically Labelled Biological Macromolecules. *Quart. Rev. Biophys 23*, 97–131.

(26) Shen, Y., Delaglio, F., Cornilescu, G., and Bax, A. (2009) TALOS+: a hybrid method for predicting protein backbone torsion angles from NMR chemical shifts. *J. Biomol. NMR 44*, 213–223.

(27) Brunger, A. T., Adams, P. D., Clore, G. M., Delano, W. L., Gros, P., Grosse-kunstleve, R. W., Jiang, J., Kuszewski, J., Nilges, M., Pannu, N. S., Read, R. J., Rice, L. M., Simonson, T., and Gregory, L. (1998) Crystallography & NMR System : A New Software Suite for Macromolecular Structure Determination. *Acta Cryst. D54*, 905–921.

(28) Pettersen, E. F., Goddard, T. D., Huang, C. C., Couch, G. S., Greenblatt, D. M., Meng, E. C., and Ferrin, T. E. (2004) UCSF Chimera--A Visualization System for Exploratory Research and Analysis. *J.Comput. Chem. 25*, 1605–1612.

(29) Kincaid, R. L., Vaughan, M., Osborne, J. C., and Tkachuk, V. a. (1982) Ca2+-dependent interaction of 5-dimethylaminonaphthalene-1-sulfonyl-calmodulin with cyclic nucleotide phosphodiesterase, calcineurin, and troponin I. *J. Biol. Chem. 257*, 10638–10643.

(30) Chen, R. F. (1968) Dansyl Labeled Proteins: Determination of Extinction Coefficient and Number of Bound Residues with Radioactive Dansyl Chloride. *Anal. Biochem. 25*, 412–416.

(31) Aoyagi, M., Arvai, A. S., Tainer, J. A., and Getzoff, E. D. (2003) Structural basis for endothelial nitric oxide synthase binding to calmodulin. *EMBO J. 22*, 766–775.

(32) Broncel, M., Wagner, S. C., Paul, K., Hackenberger, C. P. R., and Koksch, B. (2010) Towards understanding secondary structure transitions: phosphorylation and metal coordination in model peptides. *Org. Biomol. Chem. 8*, 2575–2579.

(33) Johnson, J. D., and Wittenauer, L. a. (1983) A fluorescent calmodulin that reports the binding of hydrophobic inhibitory ligands. *Biochem. J. 211*, 473–479.

(34) Mori, M., Konno, T., Ozawa, T., Murata, M., Imoto, K., and Nagayama, K. (2000) Novel Interaction of the Voltage-Dependent Sodium Channel (VDSC) with Calmodulin : Does VDSC Acquire Calmodulin-Mediated Ca 2 + -Sensitivity ? † 1316–1323.

(35) Censarek, P., Beyermann, M., and Koch, K.-W. (2002) Target recognition of apocalmodulin by nitric oxide synthase I peptides. *Biochemistry 41*, 8598–8604.

(36) Vorherr, T., Knöpfel, L., Hofmann, F., Mollner, S., Pfeuffer, T., and Carafoli, E. (1993) The calmodulin binding domain of nitric oxide synthase and adenylyl cyclase. *Biochemistry 32*, 6081–6088.

(37) Yamniuk, A. P., and Vogel, H. J. (2005) Structural Investigation into the Differential Target Enzyme Regulation Displayed by Plant Calmodulin Isoforms. *Biochemistry 44*, 3101–3111.

(38) Censarek, P., Beyermann, M., and Koch, K.-W. (2004) Thermodynamics of apocalmodulin and nitric oxide synthase II peptide interaction. *FEBS Lett. 577*, 465–468.

Table 1. Statistics for the CaM-eNOSpThr495 Peptide Structural Ensemble

	CaM-eNOSphos Complex		
NMR-derived distance and dihedral angle restraints			
NOE constraints	Calmodulin	eNOSphos peptide	CaM-eNOSphos complex
Total	1513	119	62
Dihedral angles from TALOS+	288	N/A	N/A
Total number of restraints		1982	
Structure statistics for the 20 lowest energy structures			
Mean deviation from ideal covalent geometry			
Bond lengths (Å)		0.010	
Bond angles (deg.)		1.3	
Average pairwise RMSD (Å) for all heavy atoms of the 20 lowest energy structures	All Residues	Ordered Residues[a]	Selected Residues[b]
Backbone Atoms	1.3	0.9	0.9
Heavy Atoms	1.7	1.4	1.4
Ramachandran statistics (%)			
Residues in most favored region		86.0	
Residues in additional allowed regions		13.5	
Residues in generously allowed region		0.4	
Residues in disallowed region		0.0	

[a] Ordered residue ranges: 6A-8A,10A-36A,39A-77A,79A-148A,495B-508B
[b] Selected residue ranges: 6A-8A,10A-36A,39A-77A,79A-148A,495B-508B

Table 2. Thermodynamics of CaM-Peptide Interactions Measured by ITC

	N (sites)	K_d (μM)	ΔH (kcal/mol)	ΔS (cal/mol/K)
CaM + eNOS 0.225 μM free Ca^{2+}	1.00 ± 0.01	0.2 ± 0.03	9.39 ± 0.13	62.0
CaM + eNOS 1mM free Ca^{2+}	1.02 ± 0.02	0.7 ± 0.2	-4.48 ± 0.16	13.3
CaM + eNOSpThr495 0.225 μM free Ca^{2+}	0.0096 ± 0.86*	>50	41.07 ± 369.9*	140*
CaM + eNOSpThr495 1 mM free Ca^{2+}	1.11 ± 0.01	0.3 ± 0.08	1.74 ± 0.03	35.5

*These results cannot be fit reliably by the ITC software and are indicative of poor or no binding between CaM and the eNOSpThr495 peptide.

FIGURE CAPTIONS

FIGURE 1**.** (a) Overlay of ^{1}H-^{15}N HSQC spectra of CaM-eNOS peptide complex (green) and CaM-eNOSpThr495 peptide complex (red). (b) UV-CD spectra comparison between wild type eNOS and eNOSpThr495 CaM binding peptides in buffers with varying TFE concentration. The ellipticiy at 222 nm is shown as a function of the concentration of TFE.

FIGURE 2**.** Solution structure of CaM bound to eNOSpThr495 CaM binding domain peptide. (a) Superposition of the ensemble of the 20 lowest energy structures of CaM bound to the eNOSpThr495 peptide. Backbone atom traces of CaM are shown in dark blue and the eNOSpThr495eNOS peptide are shown in light blue. (b) Cartoon ribbon view of the average solution structure of CaM-eNOSpThr495 complex. (c) Cartoon ribbon view showing residues in close proximity to the phosphorylated Thr495 of the eNOS peptide. Ca^{2+} ions are shown as green dots and are modeled in their known locations. Residues 1-40 of CaM (EF Hand I) are colored red, 41-79 (EF Hand II) are purple, 80-114 (EF Hand III) are green, and 115-148 (EF Hand IV) are blue. The peptide is colored in a lighter blue and the N and C terminus are labeled N' and C', respectively. The phosphorylated Threonine is shown as stick model.

FIGURE 3**.** Superpositions of the CaM-eNOS peptide solution structure (dark colors) and the CaM-eNOSpThr495 peptide solution structure (light colors). Comparison of solution structures of CaM-eNOSpThr495 peptide (dark colors) with CaM-eNOS peptide by superimposing the two structures and viewing it along the bound peptide from its N-terminus (N') to its C-terminus (C') on the left (front view), and rotated 90° around the horizontal axis with the N-terminus of the bound peptide on the top on the right (bottom view). The two structures are aligned by superimposing backbone atoms of the bound peptides. The color scheme is the same as figure 1.

FIGURE 4**.** The Delphi-calculated electrostatic potential maps are projected on the surface of the CaM-eNOS peptide complex (a,c) and the CaM-eNOSpThr495 peptide complex (b,d). Thr495 and pThr495 are displayed on the peptide by an * and +. The Delphi-calculated electrostatic potential maps are colored with a chimera color key ranging from (-15) red to (0) blue.

FIGURE 5. Ca^{2+} dependency of dansyl-CaM fluorescence with or without eNOS and eNOSpThr495 peptides. Normalized fluorescence is shown for CaM, CM-eNOS complex, and CaM-eNOSpThr495 under assay conditions described under Materials and Methods.

FIGURE 6. Isothermal Calorimetry (ITC) analysis indicates binding of the eNOS peptide and no binding of eNOSpThr495 peptide to CaM at physiological Ca^{2+} levels. Representative raw sample data for several CaM-peptide titrations.

FIGURES

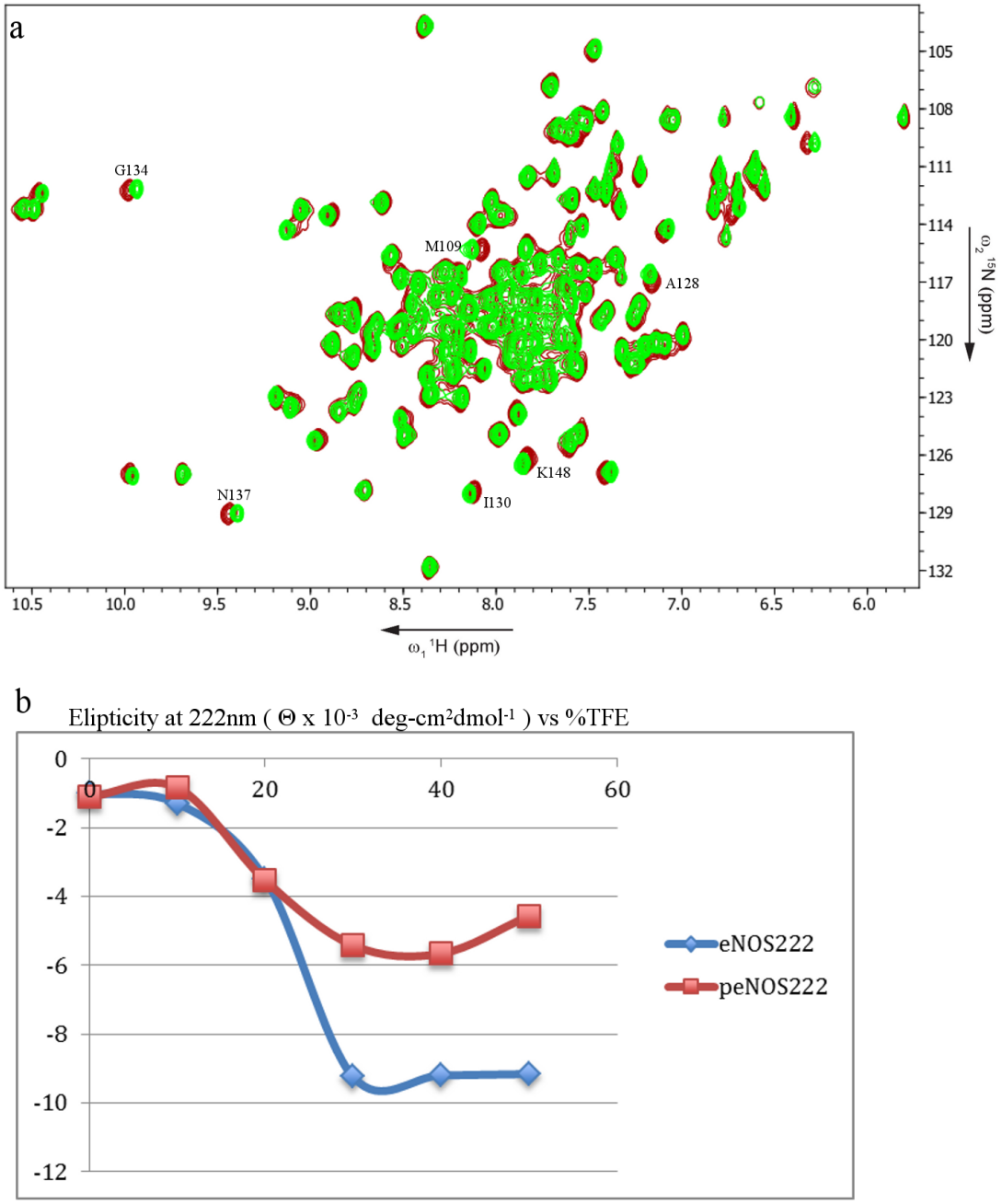

Figure 1

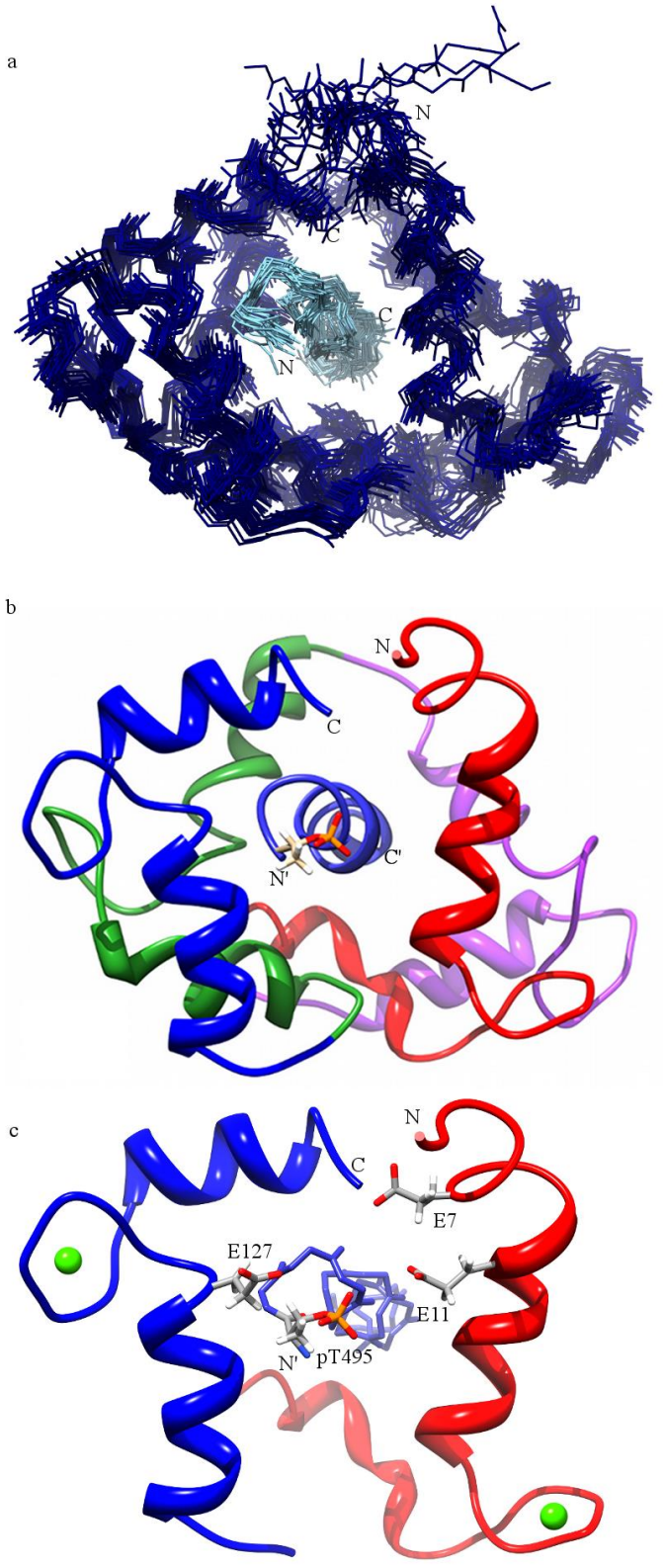

Figure 2

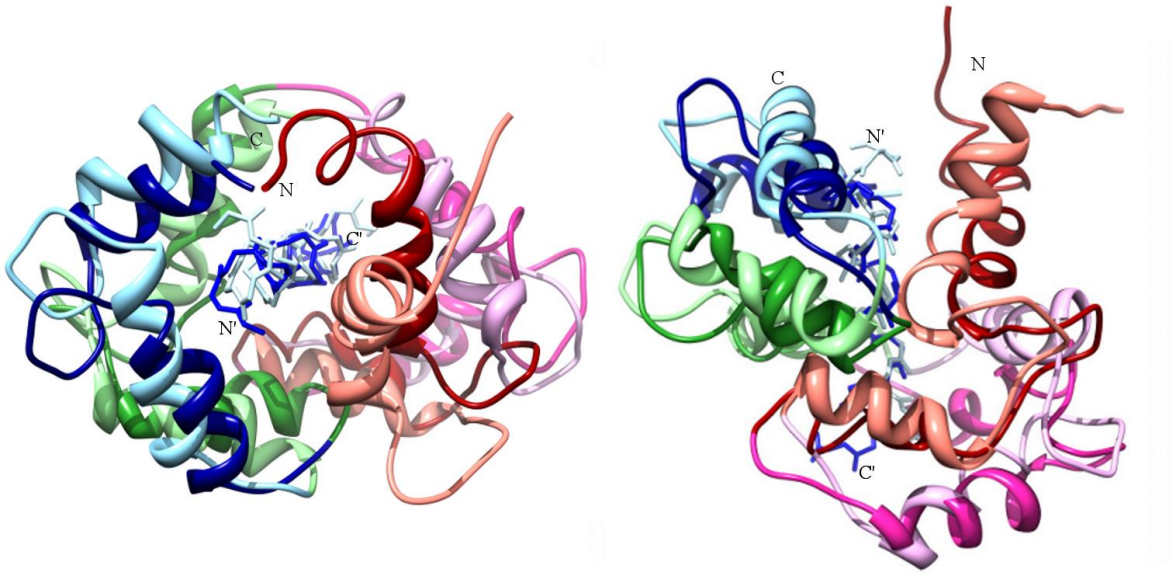

Figure 3

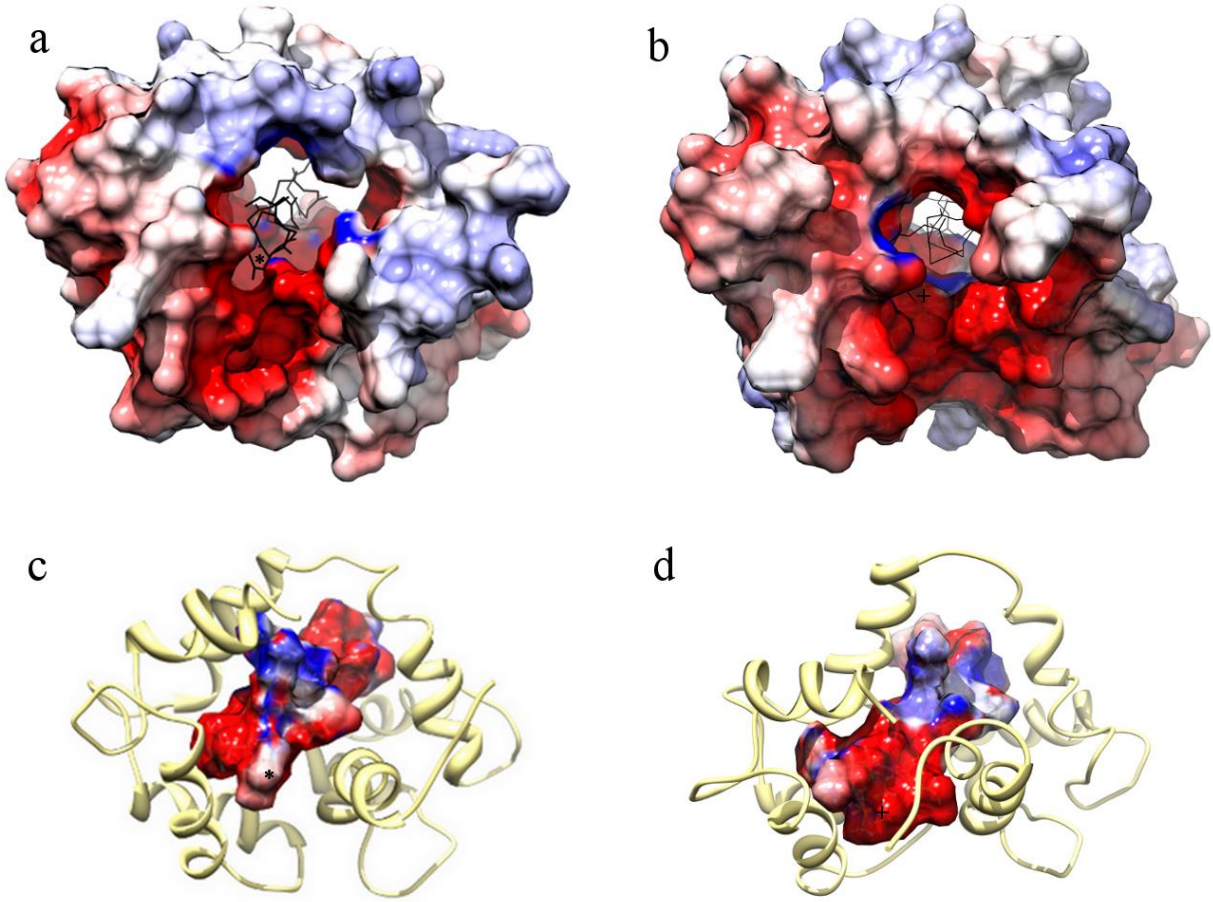

Figure 4

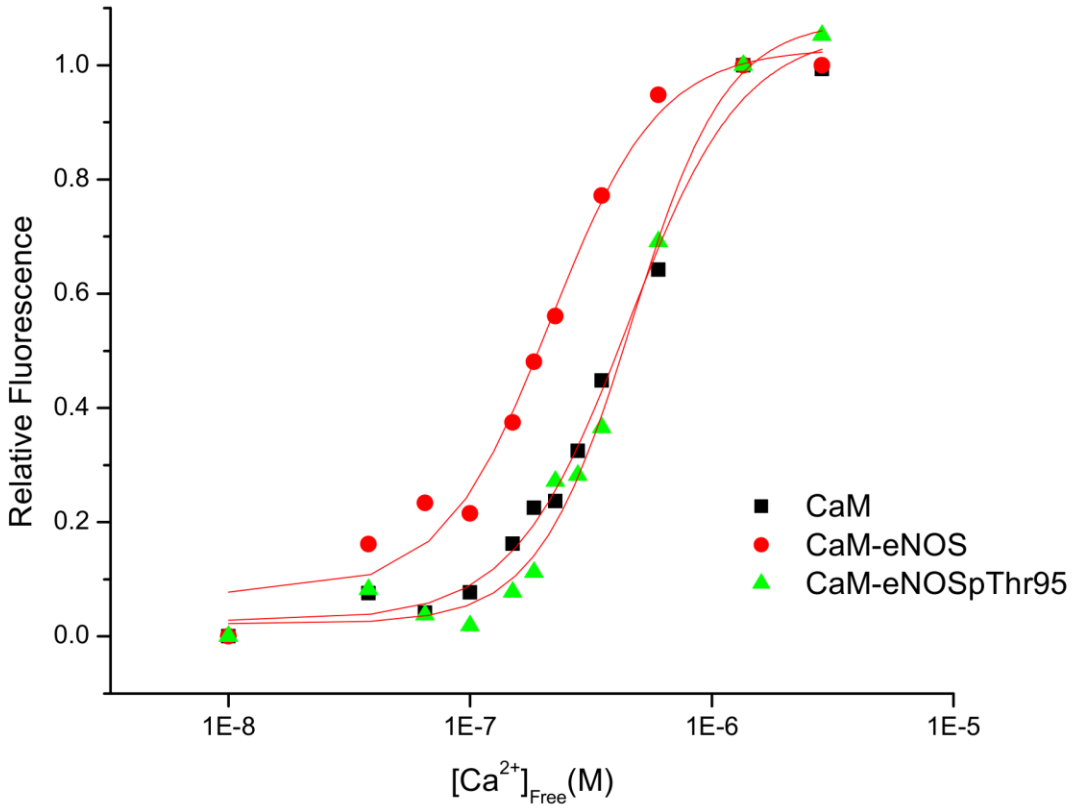
Relative Fluorescence
1.0
0.8
0.6
0.4
0.2
0.0
1E-8
1E-7
1E-6
1E-5
[Ca2+]Free(M)
CaM
CaM-eNOS
CaM-eNOSpThr95

Figure 5

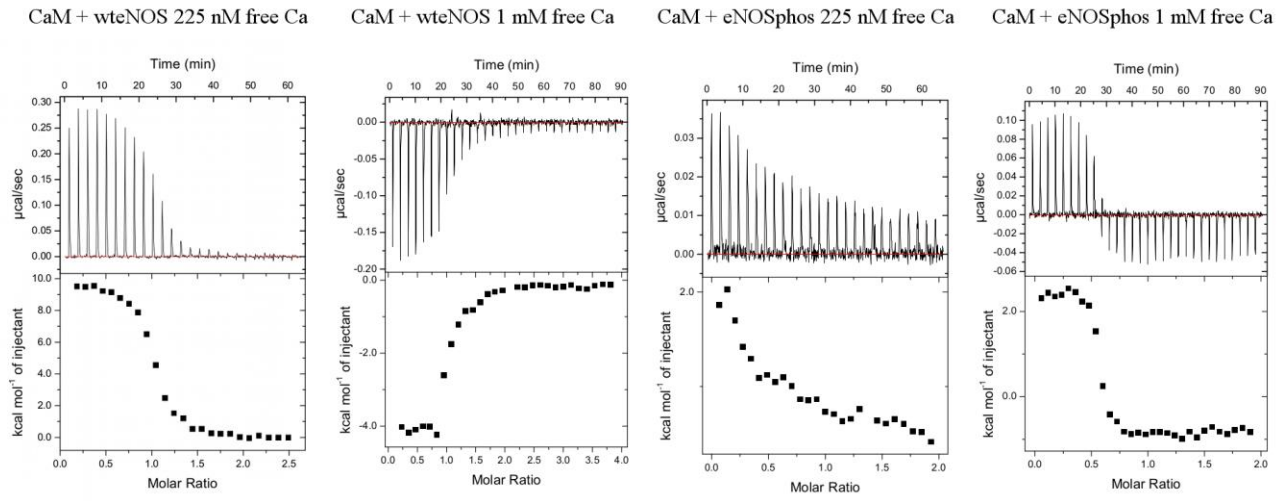
CaM + wteNOS 225 nM free Ca
CaM + wteNOS 1 mM free Ca
CaM + eNOSphos 225 nM free Ca
CaM + eNOSphos 1 mM free Ca
Time (min)
µcal/sec
kcal mol-1 of injectant
Molar Ratio

Figure 6

Graphic for Table of Contents